IEEE Access
Multidisciplinary | Rapid Review | Open Access Journal

SPECIAL SECTION ON SECURE MODULATIONS FOR FUTURE WIRELESS COMMUNICATIONS AND MOBILE NETWORKS

Received May 13, 2018, accepted July 11, 2018, date of publication July 23, 2018, date of current version August 20, 2018.

Digital Object Identifier 10.1109/ACCESS.2018.2858840

A Secure Waveform Format for Interference Mitigation in Heterogeneous Uplink Networks

QI ZENG[1,2], HAYAN NASSER[2], (Member, IEEE), AND GABRIELE GRADONI[3], (Member, IEEE)

[1]College of Electrical Engineering and Information Technology, Sichuan University, Chengdu 610065 , China
[2]Department of Electrical and Electronic Engineering, University of Nottingham, Nottingham NG7 2RD, U.K.
[3]Department of Electrical and Electronic Engineering, School of Mathematical Science, University of Nottingham, Nottingham NG7 2RD, U.K.

Corresponding author: Gabriele Gradoni (gabriele.gradoni@nottingham.ac.uk)

This work was supported in part by the National Natural Science Foundation of China under Grant 61701328 and in part by the Youth Scholar Foundation in Sichuan University under Grant 2017SCU11001.

ABSTRACT In heterogeneous networks (HetNets), providing reliable and secure transmission uplinks to combat the potential interference is a major challenge. We address the multi-tier uplink interference issue, inspired by the secure waveform design in spatial and spectral domains to improve the system reliability and capacity. A system combining a beamforming (BF) technique based on uniform circle array and a frequency-hopping (FH) technique has been developed under an orthogonal frequency division multiplex (OFDM) scheme (i.e., OFDM/FH-BF system). The modified receiver structure is designed for the hopped multi-carrier signals. The convergence of the adaptive FH-BF system, which is critical for supporting highly mobile users in HetNets, is investigated. The combined effects of FH and BF techniques on system performance, in terms of output signal-to-interference-plus-noise ratio and bit-error-rate (BER), are fully studied. The simulation results show that the proposed OFDM/FH-BF system converges in a reasonably low number of snapshots, which meets the strict requirement for serving rapidly moving users. The combination of BF and FH techniques can offer reliable uplinks by mitigating the potential interference. In particular, at the cell edge with multiple interferers K, the FH technique becomes the dominant anti-interference approach and the BER decreases with increasing size of the frequency slots set q.

INDEX TERMS Interference mitigation, OFDM/FH technique, adaptive beamforming technique, multi-tier networks, performance analysis.

I. INTRODUCTION

Heterogeneous networks (HetNets) are one of the primary solutions to improving capacity and coverage in future cellular networks [1]. HetNets consist of a conventional macro cellular (MC) deployment and overlays the small-cells (SC), including femto-and pico-cells, as shown in Fig. 1. In such an architecture, wireless transmission uplinks should be designed to protect the information from various types of threats such as eavesdropping, interception and interference. For eavesdropping and interception, cryptographic techniques are the most efficient at relieving the system degradation [2]. For interference, the design of secure waveforms in the physical layer is normally considered as the most viable solution [3].

The multi-tier interference is a critical problem in HetNet uplinks, which constitutes intra-tier and inter-tier uplink interference [4]. The intra-tier interference occurs within the small-cell or the macro-cell when the subcarrier allocations collide among multiple users. Because of the frequency reuse amongst the multi-tier in the HetNet scenario, the inter-tier interference always encounters the following types of interference: neighboring SC-user to SC-BS interference, MC-user to SC-BS interference and SC-user to MC-BS. In this paper, we only consider the multi-tier uplink interference between the SC-BS and the SC-and MC-users. Under such a multi-tier infrastructure and a ultra-dense network, the complexity of the interference problem increases significantly in HetNets.

To combat the multi-tier interference, previous studies in the literature have focused on resource scheduling solutions in the medium access control layer (MAC), such as subcarrier assignment [4] and power control [1], [5]. To implement the optimal scheduling, both methods require the global channel-state-information to coordinate with multiple points, which

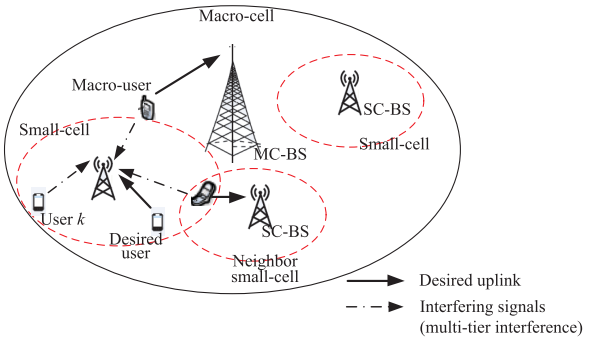

FIGURE 1. **The HetNet uplinks with multi-tier interference. The uplink networks refer to the transmission links from the desired user to its severed base station (BS), which include MC-user to MC-BS and SC-user to SC-BS.**

will increase the complexity when the multiple points belong to different operators or have conflicting utilities. Thus, in this paper, *we will explore and detail how to further suppress the interference through a physical-layer waveform technique for heterogeneous networks. The waveform solution can be used to provide secure data communication links, which can also be smoothly integrated into the MAC solutions (e.g., [1], [4] and [5]) as well as the authentication mechanisms (or encryption protocols) in the upper layer [2].*

With respect to the physical layer, we consider two potential techniques in the spatial and frequency domains, i.e., beamforming (BF) and frequency-hopping (FH), to guarantee the security and reliability in transmission links. Adaptive BF based on antenna arrays has become one of the essential techniques implemented in cellular networks due to its inherent advantages; these include robustness, antenna gain and spectrum efficiency. Also, BF can improve the efficiency in reducing interference, that is, it adjusts the value of the beam factor for each element, such that the main lobe of the antenna array points towards the desired user, and the null lobes are directed towards the interferers [6], [7]. However, due to the ultra-density and the random-movement of the users in the multi-tier networks, particularly at the cell edge, the anti-interference efficiency of BF alone is insufficient. In addition, the signals coming from the direction of the side-lobe will not be completely negated by BF and also lead to the nontrivial intra-and inter-tier interferences [8], [9].

In the spectral domain, FH is one of the most secure wireless communication technologies, which has been suggested in many promising applications such as the 5th generation (5G) cellular networks [9], Internet of Things [10] and smart grid communication infrastructure [11]. The signal frequency from the desired user is randomly hopped over a large frequency range dictated by a given FH sequence, as to avoid the narrowband interference. The FH methodology additionally facilitates users to work across multi-band, for example, hopping between 5G to 4G frequency bands, which is compatible with HetNets [12]. Hence, *combining BF and FH (so-called BF-FH) in the deployment of heterogeneous uplink networks is a promising option for the physical-layer that maintains the capacity of the network, and improves the capability to combat the multi-tier interference.*

In this paper, we will design a new FH-based adaptive BF receiver employing a uniform circle array (UCA) with N_a elements under an OFDM modulation (i.e., OFDM/FH-BF system). In the transmitter, a FH-based OFDM structure (see Fig. 2) can efficiently reduce the peak-to-average-power-ratio (PAPR) [13]. The receiver structure of the UCA pattern with $N_a = 4$ for SC-BS is shown in Fig. 3 and Fig. 4, and will be introduced in detail in Section III. As a case

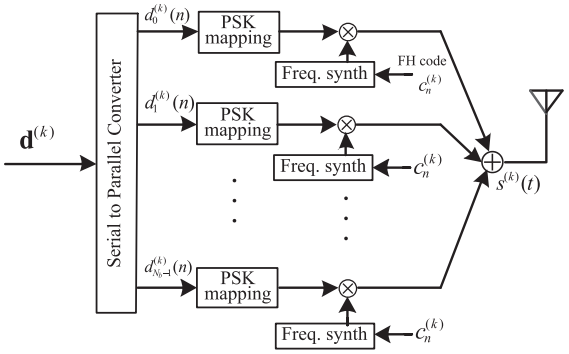

FIGURE 2. **The model of OFDM/FH transmitter with phase-shift-keying (PSK) modulation, where the binary data stream of the k-th user $\mathbf{d}^{(k)} = [d_0^{(k)}, d_1^{(k)}, \cdots, d_{N_b-1}^{(k)}]$, and $c_n^{(k)}$ denotes the assigned FH slot of the k-th user at the n-th OFDM symbol.**

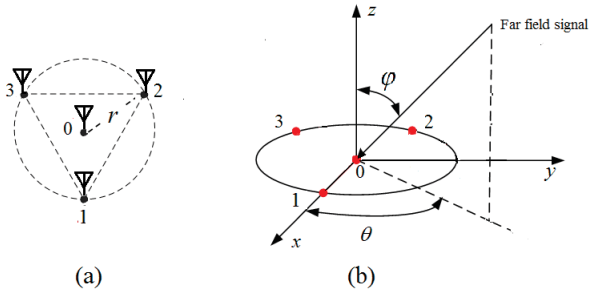

FIGURE 3. **An illustration of a UCA pattern ($N_a = 4$): (a) deployment of UCA elements; (b) direction of signal arriving at UCA.**

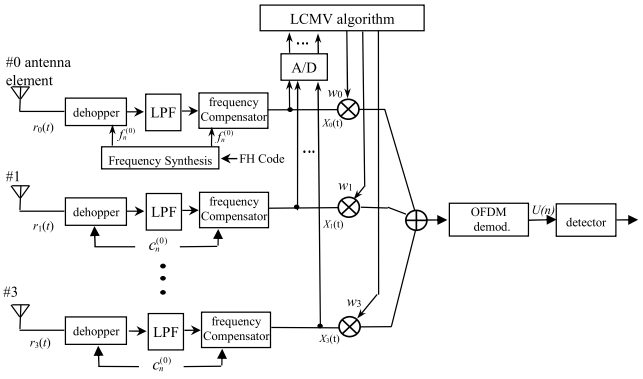

FIGURE 4. **The receiver structure of OFDM/FH-BF system for SC-BS ($N_a = 4$).**

study, the linearly constrained minimum variance (LCMV) algorithm is employed in the beamformer [6]. Subsequently, we will thoroughly reveal the behavior of convergence, output SINR and anti-interference performance of our proposed system by theoretical and numerical analysis. Particularly at the edge of the small-cells across a HetNet, the number of users (including the intended user, interferer and jammer) is normally larger than the number of degrees of freedom possible from a BF antenna (i.e., $K+1 > N_a$), and the anti-interference of BF alone could be impaired. Thus, we will also consider the performance behavior in this special case. Finally, we will verify the performance advantage of our proposed OFDM/FH-based adaptive BF system compared to the traditional OFDM/FH and OFDM-BF systems in the HetNet with multi-tier interference.

The paper is organized as follows. In Section III, the OFDM/FH-based adaptive BF transceiver model is presented in detail. In Section IV, the signal analysis of the proposed OFDM/FH-BF system is investigated, which includes interference rejection by the combination of FH and BF techniques. The analytical derivations of the output SINR and decision variables are detailed as well. In Section V, the convergence and the error-rate performance of the proposed system are demonstrated through numerical simulation. The conclusions are then drawn in Section VI.

II. RELATED WORK

In this section, we introduce the related work on the physical layer security issues in HetNets and the BF-FH system.

A. PHYSICAL LAYER SECURITY ISSUES IN HETNETS

The physical layer security offers distinct advantages compared to cryptography, making it suitable for HetNets. This is because physical layer security techniques have high scalability but do not depend on computational complexity [14]. Wang *et al.* [3] investigated the various physical layer techniques (e.g., beamforming, frequency/time allocations etc.) to safeguard the transmission links in future wireless communications, but without full technical analysis. Among these techniques, FH and pseudo-random FH-code with large linear spans are the most secure solutions to anti-interception and anti-interference [15]. Other studies on the interference mitigation in HetNets can be found in [1], [4], [5], and [16], by using resource scheduling solutions. However, these solutions require the frequent exchange of channel state information, which amplifies the complexity of the network implementation. Additionally, although the power allocation at the transmitter can be increased to ensure that the target signal-to-interference-plus-noise ratio (SINR) at the receiver is reached, using the power control methodology, other receivers from the inter-tier will be adversely affected by increased interference. Thus, it is necessary to explore a novel waveform scheme to enhance the physical layer security.

B. ORIGINAL BF-FH SYSTEM

A prototype communication system combining FH with BF techniques, based on a linear array, was originally proposed to combat the various types of jamming (e.g., partial-band jamming, following jamming etc.) [17]–[19]. However, there are some critical limitations regarding these studies when applied to HetNets. Firstly, these systems adopt low-date-rate modulations, which are not suitable to HetNets. Secondly, the adaptive BF for cellular networks should converge quickly, such that the change of beam direction can keep up with users moving at high speed. However, the mentioned studies [17]–[19] relax this criterion. Further, the previous FH-BF systems also do not take the effects of the FH parameters on transmission performance, such as the number of hopping frequencies and hit-rate, into full consideration. In fact, these parameters are essential when there are a large number of interferers at the cell edge. Both BF and FH should work together at the cell edge with a large number of interferers. In the next section, we will design and investigate a new BF-FH system which is more suitable for HetNets.

III. SYSTEM MODEL AND SIGNAL ANALYSIS

A. TRANSMITTER MODEL

A FH technique is integrated into the OFDM system with N_b branches as shown in Fig. 2, where the entire bandwidth is evenly divided into N_b non-overlapped sub-bands $\{\mathbb{F}_l, l = 0, 1, \cdots, N_b-1\}$, and each sub-band contains q frequency slots, i.e., $|\mathbb{F}_l| = q$. The active subcarrier of the l-th sub-branch is hopped within $\mathbb{F}_l$ according to a given FH sequence $\{c_n^{(k)} | k = 0, 1, \cdots, K; n = 0, 1, \cdots\}$ [13]. Due to the above hopping signal scenario, such an OFDM/FH structure can reduce the PAPR for the mobile users. For simplicity, we make the assumption that one OFDM symbol is transmitted during one hop interval; besides, all $K+1$ transmitters in multi-tier networks send the signal by the omnidirectional antenna. Then, the transmitted OFDM signal during the n-th hopping interval can be written as

$$S^{(k)}(t) = \sum_{l=0}^{N_b-1} \sqrt{2S_k} d_l^{(k)}(n) \exp\left[j2\pi t \left(\frac{c_n^{(k)}}{T} + f_l \right) \right], \quad nT \le t < (n+1)T, \quad (1)$$

where S_k is the transmitted signal power of the k-th user, and $d_l^{(k)}(n)$ denotes the baseband symbol on the l-th branch. For example, $d_l^{(k)}(n)$ is one of the symbols over the alphabet set $\{-1,1\}$ for binary phase-shift-keying (BPSK) mapping. The coefficient T denotes the interval of one OFDM symbol. $c_n^{(k)}$ denotes a FH frequency slot assigned to the k-th user at the n-th hopping interval, which is assumed to be an independently uniform-distribution for all k and n on the frequency slot set $\{1, 2, \cdots, q\}$ with size q. f_l is the first frequency slot in the l-th branch, which can be set as ql/T guaranteeing that the N_b sub-bands are not overlapped.

For the HetNet uplink, the same OFDM/FH scheme is utilized by all multi-tier users, as shown in (1), except for the specific frequencies $c_n^{(k)}$ and signal power S_k. Without any loss of generality, we consider that one desired user ($k = 0$) with signal power S_0 and K interferers from the multi-tier (including inter-and intra-tier) networks with the same power S_k, $k = 1, 2, \cdots, K$ in the networks. Thus, the signal-to-interference ratio (SIR) is equal to $SIR = S_0/S_k$, $k = 1, 2, \cdots, K$.

B. RECEIVER MODEL WITH ANTENNA ARRAY

A uniform circle array with N_a elements is employed in the receiver, where one antenna element is located at the center of the circle and the other $N_a - 1$ elements are uniformly placed on a circle with the radius r. The structure with $N_a = 4$ is presented in Fig. 3. In order to avoid the phase ambiguity between antenna elements, the radius of the UCA should be fixed as $r \leq \lambda_{\min}/2$, where $\lambda_{\min}$ represents the wavelength corresponding to the highest FH frequency, i.e., $\lambda_{\min} = 1/f_{\max} = T/(qN_b)$.

In the system, there exists one desired user with the known direction-of-arrival (DoA) of (φ_0, θ_0) with the elevation angle $\varphi_0 \in [0, \pi/2]$ and the azimuth angle $\theta_0 \in [0, 2\pi)$, while all DoAs of K interferers are unknown. The array steering vectors in response to the signal from the DoA (φ_k, θ_k) during the n-th hopping interval can be written as

$$\mathbf{a}_n^{(k)} = \begin{pmatrix} 1 \\ \exp\left(-ja_n^{(k)}\pi \sin(\varphi_k)\cos(\theta_k)\right) \\ \exp\left(-ja_n^{(k)}\pi \sin(\varphi_k)\cos(\theta_k - \frac{2\pi}{3})\right) \\ \vdots \\ \exp\left(-ja_n^{(k)}\pi \sin(\varphi_k)\cos(\theta_k - \frac{2(N_a-2)\pi}{N_a-1})\right) \end{pmatrix}, \tag{2}$$

where $a_n^{(k)} = c_n^{(k)}/(qN_b)$ represents the steering-vector fluctuation due to the hopped-frequency.

The wireless channel is assumed to be an additive white Gaussian noise (AWGN) channel. Thus, the received signal during the n-th hopping interval can be written as

$$\mathbf{r}(t) = \mathbf{A}_n \mathbf{S}(t) P(t - nT) + \mathbf{n}(t), \tag{3}$$

where $\mathbf{A}_n = \left[\mathbf{a}_n^{(0)}, \mathbf{a}_n^{(1)}, \cdots, \mathbf{a}_n^{(K)}\right]$ is a matrix of steering vectors of dimension $(N_a \times (K+1))$. Also, $\mathbf{S}(t) = \left[S^{(0)}(t), S^{(1)}(t), \cdots, S^{(K)}(t)\right]^{\mathrm{T}}$ denotes the transmitted signal vector consisting of the desired signal $S^{(0)}(t)$ and K interfering signals $\{S^{(k)}(t)|k = 1, 2, \cdots, K\}$. The coefficient $\mathbf{n}(t)$ is a vector $(N_a \times 1)$ of zero-mean complex-valued white Gaussian random variables representing the noise. $P(t - nT)$ denotes a unit rectangular function over the interval $[nT, (n+1)T)$.

The adaptive OFDM/FH-BF receiver model of the SC-BS is shown in Fig. 4, which consists of three parts: N_a receiver array branches with dehoppers, an adaptive beamformer and demodulator. In each array branch, the signals received by the array elements are firstly put into dehoppers, where local frequencies are controlled by the given FH sequence. The signals are then put into low-pass-filters (LPFs) with the bandwidth of $B_f = q/T$ and processed by a set of frequency compensators, which eliminate the steering-vector fluctuation due to the hopped-frequency. Subsequently, the signals are multiplied with the weight vector of the array by an adaptive beamformer employing the LCMV algorithm before the signals are finally put in into an OFDM demodulator. In contrast to other adaptive algorithms (e.g., least-mean-square, recursive least-square etc.), the LCVM algorithm does not require any additional reference signal except for the DoA of the desired user; thus, it will enhance the spectral efficiency. In the following section, the signals received by each array branch in the adaptive OFDM/FH-BF model are presented in detail.

IV. ANALYSIS OF OFDM/FH-BF SYSTEM

A. ANTI-INTERFERENCE BY FH

In the following analysis, we assume that the local FH carriers and FH sequence in the receiver are perfectly synchronized to those of the desired transmitter (i.e., the desired paired-transceiver $k = 0$). The desired hopping frequencies $\{c_n^{(0)}|n = 0, 1, \cdots\}$ are completely known to the transceiver. Thus, the output signal from the dehopper can be written as

$$\mathbf{X}(t) = \mathbf{r}(t)C(t), \tag{4}$$

where $C(t) = \exp(-j2\pi t c_n^{(0)}/T)$ represents the local carrier driven by the local oscillator.

As shown in (2), the array steering-vector of the beamformer is varied by the hopped-frequencies $\{c_n^{(0)}|n = 0, 1, \cdots\}$, which will lead to the inaccurate direction of the main-lobe to the desired transmitter. To address this issue, the set of frequency compensators followed with LPFs are employed in the desired receiver. Due to the fact that the desired FH sequence (i.e., $\{c_n^{(0)}\}$) is fully known for the paired transceiver, the frequency compensation is set to be $qN_b/c_n^{(0)}$. Then, the new array steering matrix after the frequency compensation is rewritten as

$$\mathbf{A}^*{}_n = \left[\mathbf{a}^{*(0)}_n, \mathbf{a}^{*(1)}_n, \cdots, \mathbf{a}^{*(K)}_n\right], \tag{5}$$

where

$$\mathbf{a}^{*(k)}_n = \begin{pmatrix} 1 \\ \exp\left(-ja_n^{(k)}\pi \sin(\varphi_k)\cos(\theta_k) qN_b/c_n^{(0)}\right) \\ \exp\left(-ja_n^{(k)}\pi \sin(\varphi_k)\cos(\theta_k - \frac{2\pi}{3}) qN_b/c_n^{(0)}\right) \\ \vdots \\ \exp\left(-ja_n^{(k)}\pi \sin(\varphi_k)\cos(\theta_k - \frac{2(N_a-2)\pi}{N_a-1}) qN_b/c_n^{(0)}\right) \end{pmatrix}. \tag{6}$$

Replacing $\mathbf{A}_n$ in (3) with $\mathbf{A}_n^*$ in (5), the output signal of the compensator during the n-th interval can be obtained as shown at the top of the this page in (7), as shown at the bottom of the next page, after some straightforward manipulation.

In (7), the first part $\mathbf{a}_n^{*(0)} D_l(t)$ is the signal contributed from the desired user at the l-th branch. The second part $I(t) = \sum_k \sum_l \delta(c_n^{(k)}, c_n^{(0)}) \mathbf{a}_n^{*(k)} I_l^{(k)}(t)$ is the signal contributed from K interferers. The third part $\mathbf{n}'(t)$ is the contribution of AWGN with the two-sided power spectral density of $N_0/2$. The function $\delta(x, y)$ is equal to 0 for $x = y$ and 1 otherwise. It is observed that $I(t) \equiv 0$ for the case when $c_n^{(k)} \neq c_n^{(0)}, k \neq 0$, which implies that all the interferers are well suppressed by the FH technique; otherwise, $I(t) \neq 0$. Consequently, the proposed system can suppress the portion of interference from the spectrum domain by the FH technique.

B. ANTI-INTERFERENCE BY BF

As discussed in the previous subsection, the other portion of interference still remains in the system for the case when $c_n^{(k)} = c_n^{(0)}$. To further improve the anti-interference capability, the digital beamformer with adaptive LCMV algorithm is employed in our system, which is as shown in Fig. 4. The LCMV algorithm is an efficient beamforming algorithm, which is described briefly as follows: Finding a weight vector $\mathbf{w} = [w_1, w_2, \cdots, w_{N_a}]^T$ such that it minimizes the output power of the LCMV beamformer under a set of linear constraints $\mathbf{C}$, that is,

$$\min_{\mathbf{w}} \ \mathbf{w}\mathbf{R}^H\mathbf{w}, \quad \text{s. t. } \mathbf{C}^H\mathbf{w} = \mathbf{e}_k, \tag{8}$$

where $[\mathbf{x}]^H$ denotes the conjugate transpose of $\mathbf{x}$. The coefficient $\mathbf{R} = \mathbb{E}\{\mathbf{X}\mathbf{X}^H\}$ denotes the covariance matrix of $\mathbf{X}(t)$. $\mathbf{C}$ is a constraint matrix $(N_a \times (K+1))$, and $\mathbf{e}_k = [0, \cdots, 0, 1, 0, \cdots, 0]^T$ is a vector $((K+1) \times 1)$ with all zeros except a one at the k-th position (assuming that the k-th user is the desired one). Thus, the optimal weight $\mathbf{w}_{opt}$ can be calculated by the following expression [6].

$$\mathbf{w}_{opt} = \mathbf{R}^{-1}\mathbf{C}(\mathbf{C}^H\mathbf{R}^{-1}\mathbf{C})^{-1}\mathbf{e}_k. \tag{9}$$

The 0-th user is assumed to be the desired user, such that it satisfies $\mathbf{C} = \mathbf{A}_n^*$ and $\mathbf{e}_0 = [1, 0, \cdots, 0]^T$. Then, the beampattern gain by the BF algorithm can be shown as

$$G(\varphi, \theta) = \mathbf{w}_{opt}^H \mathbf{a}^*(\varphi, \theta), \tag{10}$$

where $\varphi \in [0, \pi/2], \theta \in [0, 2\pi)$, and $\mathbf{a}^*(\varphi, \theta)$ is as defined in (6) omitting k and n. Based on (9), the output of the LCMV beamformer can be obtained as

$$y(t) = \mathbf{w}_{opt}^H \mathbf{X}(t). \tag{11}$$

Replacing $\mathbf{X}(t)$ with (7), the output $y(t)$ can be rewritten as

$$y(t) = \sum_{l=0}^{N_b-1} \mathbf{w}_{opt}^H \mathbf{a}_n^{*(0)} D_l(t) + \sum_{k=1}^{K} \sum_{l=0}^{N_b-1} \mathbf{w}_{opt}^H \mathbf{a}_n^{*(k)} \delta(c_n^{(k)}, c_n^{(0)}) I_l^{(k)}(t) + \mathbf{w}_{opt}^H \mathbf{n}'(t). \tag{12}$$

Generally, the covariance matrix $\mathbf{R}$ in (9) is hard to compute directly. In practice, $\mathbf{R}$ is always estimated by the finite number of samples of $\mathbf{X}(t)$, that is

$$\mathbf{X}(n_s) = \mathbf{X}(t) \mid_{t=n_s T_s'}, \tag{13}$$

where the sample interval T_s' in the analog-to-digital (A/D) model is far less than one hopping interval T. It follows that $N = \lfloor N_h T/T_s' \rfloor$ samples (known as N snapshots) can be obtained in N_h hop-intervals, where $\lfloor \cdot \rfloor$ denotes a floor function. Thus, the covariance matrix $\mathbf{R}$ is approximated by N snapshots $\mathbf{X}(n_s)$, which is denoted as

$$\hat{\mathbf{R}} = \frac{1}{N} \sum_{n_s=1}^{N} \mathbf{X}(n_s)\mathbf{X}^H(n_s). \tag{14}$$

It is well known that larger N leads to the more precise $\hat{\mathbf{R}}$, but it will consequently increase the complexity of computation and implementation.

C. ANALYTICAL OUTPUT SINR AND DECISION VARIABLES

In this subsection, the output SINR after the OFDM demodulation is firstly investigated, then the decision variables for detector are derived. For a thorough comparison, the output SINRs of two similar systems, i.e., the OFDM-BF and OFDM/FH systems [13], are studied as well. The analytical results obtained in this subsection will be used for the numerical computations and the Monte Carlo simulations in Section IV.

The OFDM demodulation consists of N_b orthogonal correlators, whose structure is as shown in [13]. Observing the correlator in the 0-th sub-branch in the following analysis, the output SINR per symbol of our proposed OFDM/FH-BF system can be calculated over the N_h possible frequency hops, which is shown as [18]

$$SINR = \frac{1}{N_h} \sum_{n=1}^{N_h} \frac{S_0 \left| \mathbf{w}_{opt}^H \mathbf{a}_n^{*(0)} D_0(t) \right|^2}{\sum_k S_k \left| \mathbf{w}_{opt}^H \mathbf{a}_n^{*(k)} \delta(c_n^{(k)}, c_n^{(0)}) I_0(t) \right|^2 + S_{\mathbf{n}} \left|\left| \mathbf{w}_{opt}^H \right|\right|^2}, \tag{15}$$

where S_0, S_k and $S_{\mathbf{n}}$ denote the desired signal power, the k-th interference power and the noise power, respectively. As a case study, the PSK mapping is employed in the transmitter, so we have $|D_0(t)| \equiv 1$ and $|I_0(t)| \equiv 1$, then the SINR can be rewritten as

$$SINR = \frac{1}{N_h} \sum_{n=1}^{N_h} \frac{S_0 \left| \mathbf{w}_{opt}^H \mathbf{a}_n^{*(0)} \right|^2}{\sum_k S_k \left| \mathbf{w}_{opt}^H \mathbf{a}_n^{*(k)} \delta(c_n^{(k)}, c_n^{(0)}) \right|^2 + S_{\mathbf{n}} \left|\left| \mathbf{w}_{opt}^H \right|\right|^2}. \tag{16}$$

Due to the orthogonality over N_b sub-branches in the OFDM, the decision variable from the 0-th correlator during the n-th

interval is considered, which is presented as

$$U(n) = \frac{1}{T}\int_{nT}^{(n+1)T} y(t)\exp\left(-j2\pi f_0\right) dt. \tag{17}$$

After some straightforward manipulation, the decision variable of the 0-th correlator can be rewritten as

$$U(n) = d_0^{(0)}(n)\sqrt{2S_0}\mathbf{a}_n^{*(0)} + \sum_{k=1}^{K}\delta(c_n^{(k)}, c_n^{(0)})\sqrt{2S_k}d_0^{(k)}(n)\mathbf{a}_n^{*(k)} + \mathbf{w}_{opt}^H\mathbf{n}'(t). \tag{18}$$

For the special case of binary PSK mapping, the decision rule dictates that the estimated symbol $\hat{d}_0^{(0)} = 0$ if $U(n) < 0$; otherwise, $\hat{d}_0^{(0)} = 1$.

In the following analysis, we will consider two similar systems (i.e., OFDM/FH system and OFDM-BF system), which are utilized for comparing the anti-interference capability with our proposed OFDM/FH-BF system. For the OFDM-BF system, the output SINR can be obtained from (16) by letting $\delta(c_n^{(k)}, c_n^{(0)}) = 1$ for all k and n, that is,

$$SINR_{OFDM-BF} = \frac{1}{N_h}\sum_{n=1}^{N_h}\frac{S_0\left|\mathbf{w}_{opt}^H\mathbf{a}_n^{*(0)}\right|^2}{\sum_k S_k\left|\mathbf{w}_{opt}^H\mathbf{a}_n^{*(k)}\right|^2 + S_{\mathbf{n}}\left|\left|\mathbf{w}_{opt}^H\right|\right|^2}. \tag{19}$$

Here, N_h is denoted as the number of OFDM symbols. For the OFDM/FH system, the output SINR can also be derived from (16), which is shown as

$$SINR_{OFDM/FH} = \frac{1}{N_h}\sum_{n=1}^{N_h}\frac{S_0}{\sum_k S_k\delta(c_n^{(k)}, c_n^{(0)}) + S_{\mathbf{n}}}. \tag{20}$$

V. SIMULATION RESULTS AND DISCUSSIONS

In this section, the performance of the proposed OFDM/FH-BF system is investigated under the multi-tier interference. The effects of the FH parameters (e.g., the number of frequency slots q) and BF parameters (e.g., the number of snapshots N) on anti-interference performance are revealed by the numerical and simulation results. Furthermore, the convergence rate of the proposed OFDM/FH-BF system is demonstrated in terms of average SINR. The bit-error-rate (BER) of the proposed system is evaluated based on the decision variable expression (18). To demonstrate the performance advantage, a comparison of performance between our proposed OFDM/FH-BF, and the existing OFDM/FH and OFDM-BF systems is presented in this section.

The simulation parameters are set as shown in Table 1. We simulate one MC overlaid by three SCs with multiple users that are randomly and uniformly dropped in each cell. The intended uplink is subject to the multi-tier interference, i.e., MC-and SC-users to SC-BS interference. The maximum transmit powers at SC-and MC-users are fixed to 10 dBm and 30 dBm respectively, and the AWGN power density is set to be -174 dBm/Hz. FH patterns (FH code sets) are generated by following the uniform-distribution over q frequency slots. System bandwidth is taken as 20 MHz. The wireless channel is considered as a Rayleigh fading channel, in which the path-loss model is as shown in Tab. 1.

TABLE 1. Simulation parameters.

Parameters	Values
Cell layout	Hexagonal grid
Number of macro-cell	1
Number of small-cell	3
Radius of small-cell	50 m
Radius of macro-cell	500 m
Frequency carrier	2.5 GHz
Bandwidth	20 MHz
Number of OFDM subcarries	256
FH pattern	Uniformly random hopping over q frequency slots
SC-BS antenna gains	0 dBi
Max. Tx power of MC-users	30 dBm
Max. Tx power of SC-users	10 dBm
AWGN power density	-174 dBm/Hz
MS-and SC-users distribution	Uniformly random distribution
Path loss model (in dB)	$15.3 + 37.6\log_{10} d$ with d in meters
Shadowing model	Log-normal shadowing

Fig. 5 demonstrates the antenna beam-pattern of our OFDM/FH-BF system based on the UCA structure with $N_a = 4$, where the vertical axis denotes the normalized beam-pattern gains of the beamformer (referring to (10)). In the simulation, we assume that the DoA from the desired user is $(\varphi_0, \theta_0) = (50°, 80°)$ and those of the two interferers ($K = 2$) are $(\varphi_{1,2}, \theta_{1,2}) = \{(35°, 230°), (25°, 310°)\}$. From Fig. 5, it is observed that the UCA can form a 3-dimensional beam pattern with the elevation and azimuth angles, which is more suitable for the HetNet than a uniform-linear-array pattern. The DoA of the main lobe is directed towards the desired user, while the null-lobes are directed towards the interfering users.

The output SINRs of the proposed OFDM/FH-BF system are plotted in Fig. 6 by computing (16). The parameters are set as: $q = 20$, SNR $= 8$ dB, SIR $= -10$ dB. These curves also indicate the convergence of the adaptive LCMV algorithm in our OFDM/FH-BF system versus the

$$\mathbf{X}(t) = \sum_{l=0}^{N_b-1}\mathbf{a}_n^{*(0)}\sqrt{2S_0}d_l^{(0)}(n)\exp\left(j2\pi tf_l\right) + \sum_{k=1}^{K}\sum_{l=0}^{N_b-1}\delta(c_n^{(k)}, c_n^{(0)})\mathbf{a}_n^{*(k)}\sqrt{2S_k}d_l^{(k)}(n)\exp\left(j2\pi f_l t\right) + \mathbf{n}'(t)$$
$$= \sum_{l=0}^{N_b-1}\mathbf{a}_n^{*(0)}D_l(t) + \sum_{k=1}^{K}\sum_{l=0}^{N_b-1}\mathbf{a}_n^{*(k)}\delta(c_n^{(k)}, c_n^{(0)})I_l^{(k)}(t) + \mathbf{n}'(t) \qquad nT \le t < (n+1)T \tag{7}$$

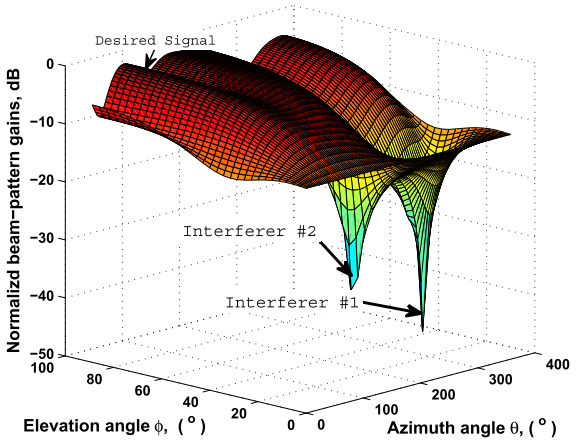

FIGURE 5. Antenna beam-pattern gains of the proposed system based on the UCA structure ($N_a = 4$, $K = 2$).

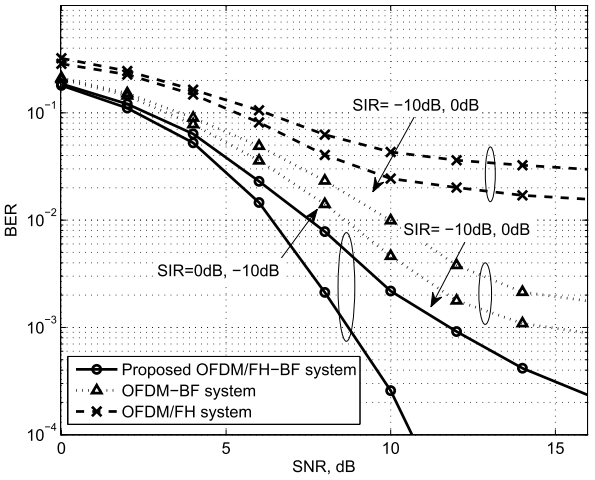

FIGURE 7. BERs of OFDM/FH-BF system for various SIRs and $K = 2$.

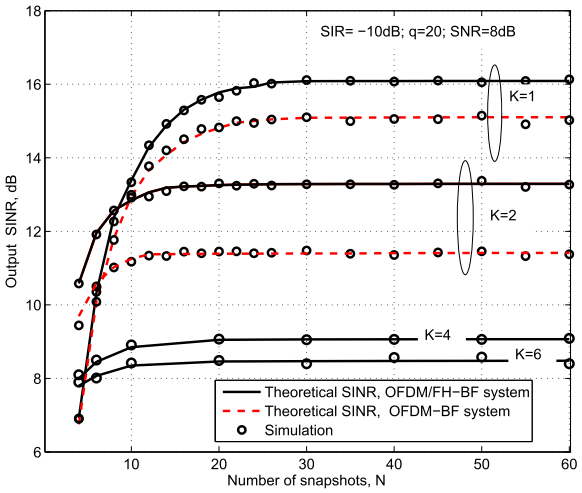

FIGURE 6. Output SINRs of OFDM/FH-BF system for various Ks, SIR $= -10$ dB.

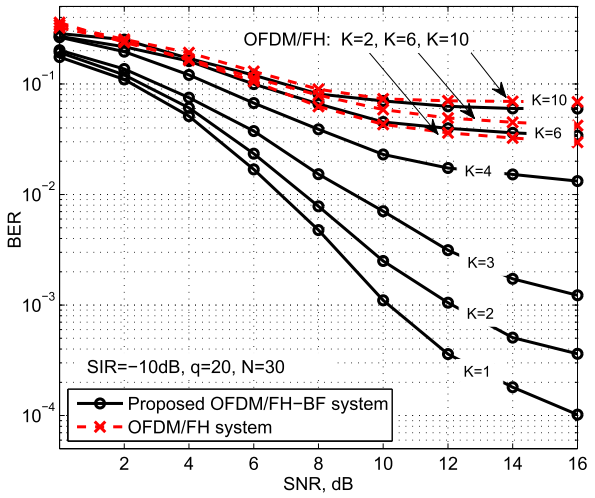

FIGURE 8. BER of OFDM/FH-BF system versus SNR for various Ks.

number of snapshots (N). From this figure, the output SINR can achieve a stable value as N increases, and the proposed system can converge within a small value of N between $20 \sim 30$ snapshots, while in previous studies [17]–[19], the convergence rate N normally takes between $100 \sim 1000$ snapshots. Due to the combination of FH and BF techniques utilized in the proposed system, considerable gains in the SINR at convergence are offered over FH and BF independently. However, for the special case of $K + 1 > N_a = 4$, the array antenna cannot provide enough degrees of freedom to cancel the interferers, and consequently the output SINR notably degrades. The theoretical results in (16) and (19) are validated by simulations.

The BERs of the OFDM/FH-BF system for various SIRs are shown in Fig. 7. The figure also shows the BER comparisons between our system and the independent FH and BF systems. The parameters are set to be same as those in Fig. 6. In an environment where the interference is considerable and with the same SIR, the proposed OFDM/FH-BF system achieves the best anti-interference performance amongst these systems under comparison. The OFDM/FH and the OFDM-BF systems are inferior at suppressing the interference individually. From this figure, we can conclude that the combination of BF and FH offer greater gains in SINR than FH or BF alone.

In Fig. 8, the BER of the proposed OFDM/FH-BF system for various values of K are plotted. In the figure, the curves agree with the traditional behavior, that is, the BER degrades with increasing K. At the edge of the small-cell, where the active interferers served by the macro-cell and neighboring small-cells are crowded due to mobility, we consider the anti-interference capability of the proposed system in the case of $K + 1 > N_a$. In such a case, the performance mainly depends on the FH technique rather than the BF technique, but the BER of the proposed system performs better than the OFDM/FH system alone. As K increases beyond 10, it can be deduced that the BER of our proposed

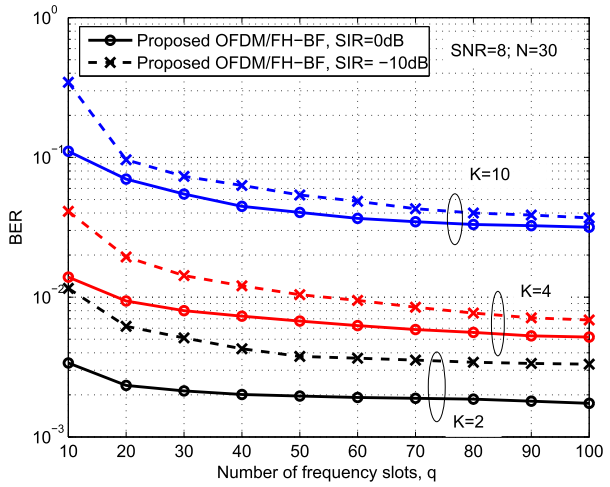

FIGURE 9. Impacts of the number of frequency slots q on the BERs of the proposed systems with SNR = 8 dB, SIR = 0 dB and −10 dB.

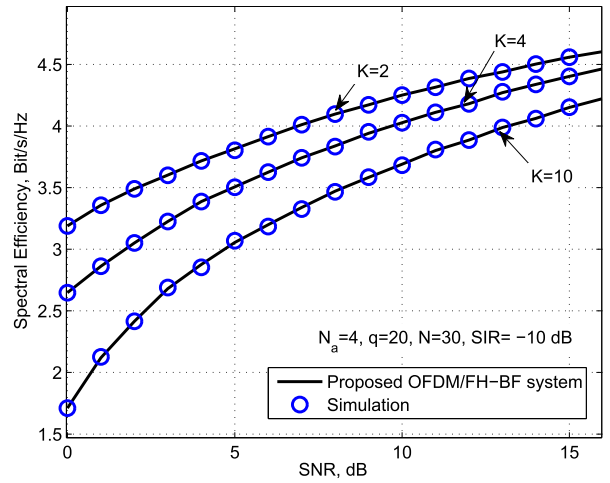

FIGURE 10. The spectral efficiency of our proposed system for a SC-user versus SNR in uplinks (N_a=4, q=20, SIR = −10 dB).

OFDM/FH-BF system will tend towards that of the OFDM/FH system.

The impact of the number of frequency slots q on the OFDM/FH-BF system for SIR = 0 dB and −10 dB are plotted in Fig. 9. The active frequencies $\{c_n^{(k)}|k = 0, 1, \cdots, K; n = 0, 1, \cdots\}$ are independently and randomly selected over the frequency slot set $\{1, 2, \cdots, q\}$. It is observed that the BER performance improves as q increases. This is because the larger frequency-range of the FH results in the lower hit-rate of $\delta(c_n^{(k)}, c_n^{(0)}) = 1$ and consequently this leads to less interference. This phenomenon can be also explained by looking at (16). Fig. 9 shows that when $K + 1 > N_a$, the proposed system can obtain the desired BER level by increasing q or by scheduling the orthogonal hopping-pattern [20].

In Fig. 10, we plot the spectral efficiency of our proposed system for a SC-user versus SNR in uplinks. We consider a possible antenna configuration in the typical deployment: one transmitting and four receiving antennas, and the frequency hopped randomly over q frequency slots ($q = 20$). It is found that the spectral efficiency decreases with increasing number of total SC-and MC-users K, due to the existence of multi-tier interference, but the spectral efficiency is still well within an acceptable level at the cell edge. The simulation and theoretical results agree well.

VI. CONCLUSION

In this paper, we have thoroughly investigated a secure waveform scheme, i.e., an OFDM/FH-based array antenna infrastructure, in order to improve the reliability of transmission uplinks in HetNet. A modified beamforming receiver structure based on a UCA pattern has been designed for wide-band OFDM/FH signals. The convergence rate of an adaptive BF algorithm was discussed. The impact of the FH parameters and BF parameters (e.g., the number of frequency slots q, the number of interferers K, the number of snapshots N, SNR and SIR) on system performance, in particular at the cell edge with multiple interferers, were studied via theoretical and numerical simulation analysis.

The analysis in this paper shows that the proposed OFDM/FH-BF system with adaptive LCMV algorithm converges in a small number of snapshots N, which implies that the adaptive BF control could be implemented perfectly during the short hopping interval, and can keep up with the direction change of the highly mobile users. The proposed system can significantly reduce the interference by using the combination of FH and BF techniques, compared with the OFDM/FH and OFDM-BF systems independently. The spectral efficiency for the SC-user can be maintained at a desirable level. Additionally, at the cell edge, where the total number of users is usually larger than the number of antenna elements ($K + 1 > N_a$), the proposed system can achieve acceptable BER and spectral efficiency. Results obtained in this paper provide a promising physical layer solution to enhance the security in heterogeneous uplink networks, which could be integrated with other interference management and encryption protocols in the upper layers.

REFERENCES

[1] E. Hossain, M. Rasti, H. Tabassum, and A. Abdelnasser, "Evolution toward 5G multi-tier cellular wireless networks: An interference management perspective," *IEEE Wireless Commun.*, vol. 21, no. 3, pp. 118–127, Jun. 2014.

[2] X. Duan and X. Wang, "Authentication handover and privacy protection in 5G HetNets using software-defined networking," *IEEE Commun. Mag.*, vol. 53, no. 4, pp. 28–35, Apr. 2015.

[3] Y. Wang, Z. Miao, and L. Jiao, "Safeguarding the ultra-dense networks with the aid of physical layer security: A review and a case study," *IEEE Access*, vol. 4, pp. 9082–9092, Dec. 2016.

[4] Y. Sun, R. P. Jover, and X. Wang, "Uplink interference mitigation for OFDMA femtocell networks," *IEEE Trans. Wireless Commun.*, vol. 11, no. 2, pp. 614–625, Feb. 2012.

[5] T. K. Vu, M. Bennis, S. Samarakoon, M. Debbah, and M. Latva-Aho, "Joint load balancing and interference mitigation in 5G heterogeneous networks," *IEEE Trans. Wireless Commun.*, vol. 16, no. 9, pp. 6032–6046, Sep. 2017.

[6] A. Sharma and S. Mathur, "Performance analysis of adaptive array signal processing algorithms," *IETE Tech. Rev.*, vol. 33, no. 5, pp. 472–491, May 2016.
[7] S. Chen, S. Sun, Q. Gao, and X. Su, "Adaptive beamforming in TDD-based mobile communication systems: State of the art and 5G research directions," *IEEE Wireless Commun.*, vol. 23, no. 6, pp. 81–87, Dec. 2016.
[8] Z. Zhang, K. C. Teh, and K. H. Li, "Performance analysis of two-dimensional massive antenna arrays for future mobile networks," *IEEE Trans. Veh. Technol.*, vol. 64, no. 11, pp. 5400–5405, Nov. 2015.
[9] D. Torrieri, S. Talarico, and M. C. Valenti, "Analysis of a frequency-hopping millimeter-wave cellular uplink," *IEEE Trans. Wireless Commun.*, vol. 15, no. 10, pp. 7089–7098, Oct. 2016.
[10] Z. Bai, B. Li, M. Yang, Z. Yan, X. Zuo, and Y. Zhang, "FH-SCMA: frequency-hopping based sparse code multiple access for next generation Internet of Things," in *Proc. IEEE Wireless Commun. Netw. Conf. (WCNC)*, San Francisco, CA, USA, Mar. 2017, pp. 1–6.
[11] Q. Zeng, H. Li, and D. Peng, "Frequency-hopping based communication network with multi-level QoSs in smart grid: Code design and performance analysis," *IEEE Trans. Smart Grid*, vol. 3, no. 4, pp. 1841–1852, Dec. 2012.
[12] S. Niknam, A. A. Nasir, H. Mehrpouyan, and B. Natarajan, "A multiband OFDMA heterogeneous network for millimeter wave 5G wireless applications," *IEEE Access*, vol. 4, pp. 5640–5648, Oct. 2016.
[13] M. Ebrahimi and M. Nasiri-Kenari, "Performance analysis of multicarrier frequency-hopping (MC-FH) code-division multiple-access systems: Uncoded and coded schemes," *IEEE Trans. Veh. Technol.*, vol. 53, no. 4, pp. 968–981, Jul. 2004.
[14] N. Yang, L. Wang, G. Geraci, M. Elkashlan, J. Yuan, and M. Di Renzo, "Safeguarding 5G wireless communication networks using physical layer security," *IEEE Commun. Mag.*, vol. 53, no. 4, pp. 20–27, Apr. 2015.
[15] J. Jung and J. Lim, "Chaotic standard map based frequency hopping OFDMA for low probability of intercept," *IEEE Commun. Lett.*, vol. 15, no. 9, pp. 1019–1021, Sep. 2011.
[16] S. Bassoy, M. Jaber, M. A. Imran, and P. Xiao, "Load aware self-organising user-centric dynamic comp clustering for 5G networks," *IEEE Access*, vol. 4, pp. 2895–2906, 2016.
[17] K. T. Wong, "Acoustic vector-sensor FFH 'blind' beamforming & geolocation," *IEEE Trans. Aerosp. Electron. Syst.*, vol. 46, no. 1, pp. 444–448, Jan. 2010.
[18] Y. Kamiya and O. Besson, "Interference rejection for frequency-hopping communication systems using a constant power algorithm," *IEEE Trans. Commun.*, vol. 51, no. 4, pp. 627–633, Apr. 2003.
[19] N. Alagunarayanan, F. Liu, and C. C. Ko, "Least squares symbol detection for two-antenna frequency hopping/M-ary frequency shift keying systems in the presence of follower jamming," *IET Signal Process.*, vol. 6, no. 8, pp. 781–788, Oct. 2012.
[20] Q. Zeng and X. Liu, "Chaos theory-based NHZ-FH sequence set for quasi-synchronous FHMA system," *Electron. Lett.*, vol. 53, no. 22, pp. 1493–1495, Sep. 2017.

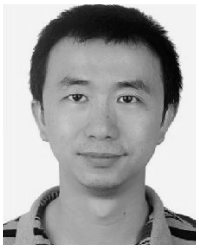

QI ZENG received the Ph.D. degree in communication and information system from Southwest Jiaotong University, Chengdu, China, in 2012. From 2010 to 2012, he was a Visiting Ph.D. Student with the University of Tennessee, Knoxville, USA. In 2016, he joined the College of Electrical Engineering and Information Technology, Sichuan University, China, as a Lecturer. He is currently a Visiting Scholar with the Department of Electrical and Electronic Engineering, University of Nottingham, U.K.

His research interests include multiple-carrier systems, interference cancelation, antenna array processing, and 5G cellular networks. He is a Reviewer of the IEEE COMMUNICATION LETTER, the IEEE TRANSACTIONS ON INDUSTRIAL ELECTRONICS, *IET Networks*, *IET Communication*, and the *Journal of Wireless Communications*, and *Mobile Computing*.

HAYAN NASSER (M'16) received the master's degree (Hons.) and the Ph.D. degree in electrical and electronic engineering from the University of Nottingham in 2011 and 2015, respectively. He has been a Post-Doctoral Researcher with the University of Nottingham since 2015.

His research interests involve computational electromagnetics and very large scale meshing and modeling for the purposes of electromagnetic simulation, with applications primarily in communications and the next generation wireless technologies.

GABRIELE GRADONI (M'11) received the Ph.D. degree in electromagnetics from the Universita' Politecnica delle Marche, Ancona, Italy, in 2010. In 2008, he was a Visiting Researcher with the Time, Quantum, and Electromagnetics Team, National Physical Laboratory, Teddington, U.K. From 2010 to 2013, he has been a Research Associate with the Institute for Research in Electronics and Applied Physics, University of Maryland, College Park, USA. From 2013 to 2016, he was a Research Fellow with the School of Mathematical Sciences, University of Nottingham, U.K. Since 2016, he has been an Assistant Professor of mathematics and electrical engineering with the University of Nottingham.

His research activity is in probabilistic and asymptotics methods for propagation in complex wave systems, wave chaos, and MIMO wireless systems. He is a member of the American Physical Society, and the Italian Electromagnetics Society. He was a recipient of the URSI Commission B Young Scientist Award in 2010 and 2016 and the Gaetano Latmiral Prize in 2015. Since 2014, he has been the URSI Commission E Early Career Representative.